Eur. Phys. J. D **26**, 73–77 (2003)
DOI: 10.1140/epjd/e2003-00246-x

THE EUROPEAN PHYSICAL JOURNAL D

High-intensity lasers and controlled fusion

R.R. Freeman[1,a], C. Anderson[1], J.M. Hill[1], J. King[1], R. Snavely[1], S. Hatchett[2], M. Key[2], J. Koch[2], A. MacKinnon[2], R. Stephens[3], and T. Cowan[3]

[1] Department of Applied Science, University of California, Davis, CA, USA
[2] Lawrence Livermore National Lab, University of California, Livermore, CA, USA
[3] General Atomics, San Diego, CA, USA

Received 22 November 2002
Published online 5 August 2003 – © EDP Sciences, Società Italiana di Fisica, Springer-Verlag 2003

Abstract. The use of high-intensity lasers to cause ignition in inertial confinement fusion is presented, with emphasis on current experimental programs and physical concepts that are at the forefront of the field. In particular, we highlight the issues of fast electron transport through dense materials, an essential element of the "Fast Ignitor" concept.

PACS. 52.20.Fs Electron collisions – 52.38.Kd Laser-plasma acceleration of electrons and ions

1 Introduction

Fusion energy has the potential for the generation of essentially limitless energy without the drawbacks of global warming from burning carbon-based fuels, nor the storage of dangerous reaction products from fission energy processes. The idea of controlled fusion "burn" has been around since the demonstration of the first fusion energy "thermonuclear" bomb in 1955. It has had a long and frustrating research history, centered largely on the concepts of dilute plasmas being confined at high temperatures with various configuration of magnetic fields. This research goes by the name of magnetic confinement fusion (MFE) and still, today, has a large number of researchers in the field. The problem has always been that the dilute plasma must be confined for significant times (seconds) at high temperature. Substantial progress has been made on this technique despite the numerous instabilities inherent in such plasmas confinement.

There is another direction that fusion energy research has taken: inertial confinement fusion (ICF): a technique that relies upon the compression of small quantities of deuterium/tritium, usually in a pellet, to very high densities by high-energy laser pulses in a manner that also creates a high-temperature core. If appropriate conditions can be met, the D/T should undergo fusion, and the process is said to have "ignited" [1]. The problem has always been that the required laser intensities and symmetry conditions have frustrated the realization of this process up to this time also [2].

The latest in the evolution of laser inertial confinement fusion on ICF that has its origins in the basic high-field laser-matter interactions pioneered by the ICOMP community. The new technique separates the compression of the pellet from the heating. In so doing, the requirements on the compression laser, both in intensity and symmetry, are greatly relaxed. The difficulties are, of course, transferred to the heating pulse, which is envisioned as an ultra-intense, sub picosecond laser pulse that will deposit the requisite heating energy in the short time the pellet is confined by its inertia [3]. This idea, which goes by the name "Fast Ignitor", has gained a lot of attention recently [4,5]; in this paper we outline the proposal and discuss recent experiments on the transport of high-energy electrons (created within the laser/matter interaction zone) through dense material [6,7].

2 Concepts

Standard inertial confinement fusion (ICF) relies on what is known as "isobaric" compression of a pellet (see Fig. 1): in this case, the pellet is designed with a higher-density shell and a low-density interior, both made of deuterium and tritium. When the pellet is compressed (either with the direct application of visible lasers- "direct drive", or the application of intense X-rays generated by visible light on an outer balloon-like structure (hohlraum) that surrounds the pellet (so-called "Indirect Drive"), the pressure is uniform, and since the temperature T times the density ρ is a constant, a low density, high temperature central core spot develops that supposedly reaches ignition temperature (on the order of many keV).

Although the detailed parameters for ignition of D-T pellets using isobaric ignition are considered to be well established [8], such is not the case for isochoric (constant

[a] e-mail: rrfree@ucdavis.edu

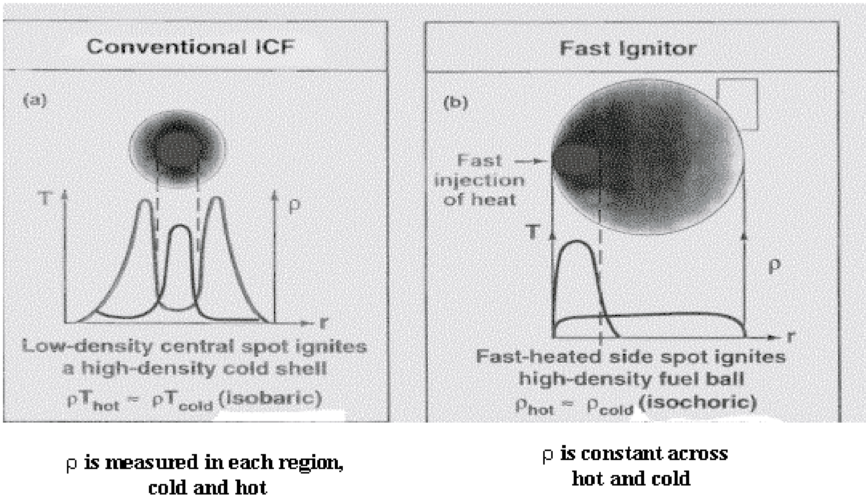

Fig. 1. The difference between isobaric compression of a capsule on varying density and the isochoric heating of a constant density target.

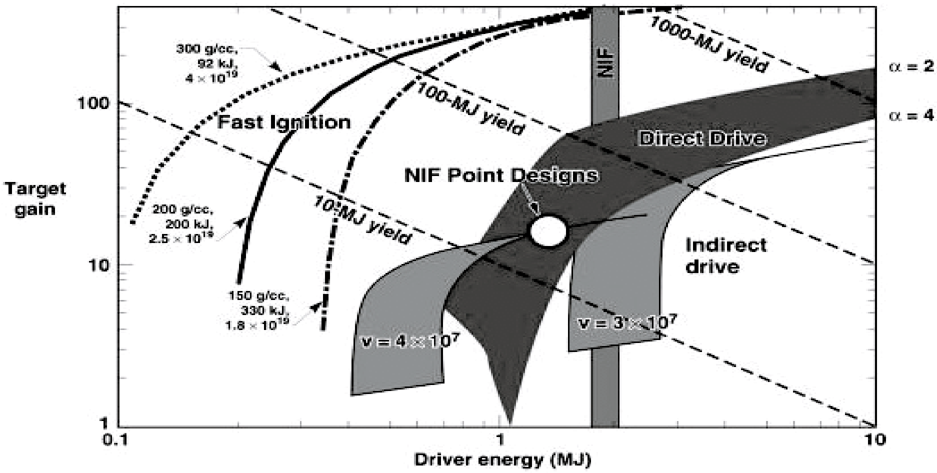

Fig. 2. Target gain for the national ignition facility (calculated).

density) ignition with "Fast Ignition" (FI). The generalities of FI have been known for 10 years [4]. In contrast to the conventional ICF, using FI, the target is first compressed to an uniform density (isochoric) at the required density (on the order of 200 gm/cm^3) by either direct or indirect drive. The ignition is initiated by a fast pulse laser, which "bores" through the outer lower density edges of the target, then deposits its energy into fast electrons (∼MeV) near the relativistic critical density surface [9]. The aerial density for ignition at the core ($\rho R \sim 0.3$ g/cm^2) is set by the 3.5 MeV α particle range in D-T, which must be matched by the 1 MeV electron energy deposition; further the required ignition energy is independent of target size, and scales only as the density of the target as $\rho^{-1.85}$.

For the assumption that the ignition threshold corresponds to a target size equal to the ignition spark size, while larger targets require proportionally more compression energy, the ignition energy remains constant. Thus gain in FI can be considerably larger than in conventional ICF because lower fuel density can be used with an acceptable ignition threshold (for example: assuming a relatively modest transport efficiency of energy from the FI ignition laser, a 100 kJ pulse of time duration 10 ps can deliver the required ignition spark of 35 kJ to a 30 μm radius spot in a 200 g/cm^3 target). For larger systems, with the same FI transport efficiency, a 1 MJ total input energy-90% of which is used for compression-would yield a gain of over 300 in a D-T target. Figure 2 shows target gain *vs.* laser driver energy [5]. (Here target gain is defined as the ratio of the energy released in the D-T reactions within the target divided by the total laser input energy) Isobaric central spark indirect drive (including the National Ignition Facility at LLNL point design) and direct drive are shown for comparison with isochoric ignition for fuel densities of 150, 200, and 300 g/cm^3. Labels indicate compressed fuel density, FI laser pulse energy and ($I\lambda^2$). It is clear from Figure 2 that the opportunity to greatly increase the "yield" using FI over conventional ICF is apparent.

FI requires a target with pure DT in the igniting volume, and a well-connected isochoric fuel mass. Since the density and pressure are less than in isobaric compression, they are, in principle easier to obtain, and presumably considerably less susceptible to hydrodynamic instabilities. Since the conventional central hot spot is not required, the bulk of the fuel does not have strict requirements for composition or for shape. By decoupling the implosion from the ignition, a potential fusion system could use lasers,

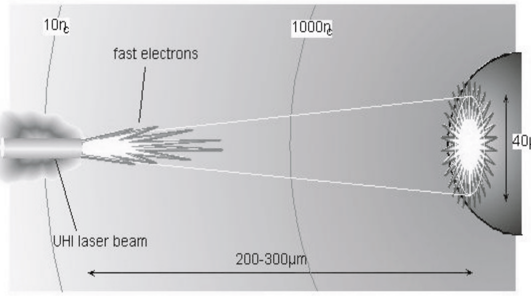

Fig. 3. "Hole Burning" of the ultra-high intense laser to the relativistic critical surface, where nearly 30% of the laser energy is converted to fast electrons. The fast electrons must stay relatively collimated through vastly increasing densities to hit the compressed core.

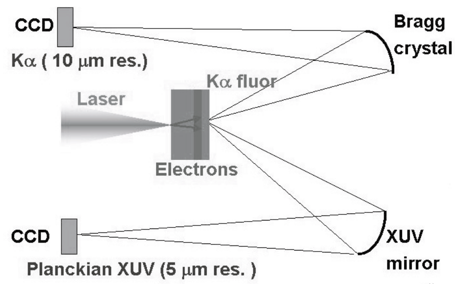

Fig. 4. The experimental set-up. The crystals are bent circularly, and the angles in this picture are greatly exaggerated. To avoid image distortions, the actual opening angles are held to be on the order of one degree.

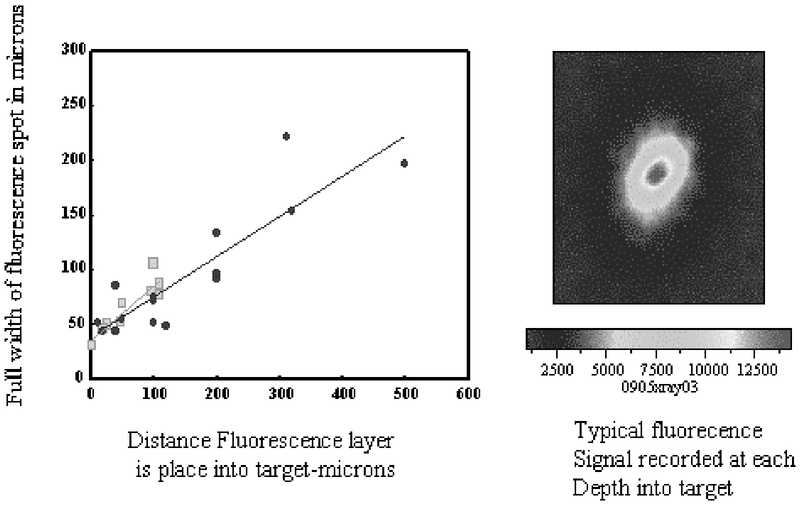

Fig. 5. An important result of our measurements. The fluorescence signals from the buried layers were recorded at both the LULI laser and the RAL laser. Typical fluorescence patterns are shown. When all the data is plotted, the widths are seen to increase at a full angle of ∼40 degrees. More importantly, the width does not approach the laser spot size even when the fluorescence layer is placed at the very front of the target.

ion beams or even sophisticated "Z-pinches" in various direct/indirect configurations, while reserving the ignition for the FI short pulse laser.

While there is substantial evidence of high efficiency (> 30%) conversion of intense pulse energy into fast electrons at the critical surface of a target [9], there remains the crucial question of the efficiency of transport of these electrons to the core region. The critical surface is pushed inward by the light pressure, and develops at a higher than usual density due to relativistic effects [10]. In the naive FI scheme, the generated fast electrons at this critical surface are presumed to travel in a tight cone inwards through over nearly 4 orders of magnitude increase in density to the ∼200 g/cm^3 core, where they lose their energy in a stopping distance approximating the α particle range of the D-T thermonuclear reaction [4,6,11]. Figure 3 is a diagram indicating the essential physics. The fundamental issue here is that there is no clear experimental evidence, nor any reliable modeling/theory, that indicates in what distribution (in phase space) the fast electrons are created, nor how these electrons will, in fact, propagate through this rapidly spatial varying density. Thus, FI remains a "CONCEPT" exploration, precisely because of these crucial uncertainties.

3 Summary of recent experimental work

These experimental results come from two experimental campaigns of the authors over the last year. We have developed X-ray and XUV imaging diagnostics for simultaneous multiple views of electron transport and heating profiles in solid density plasmas (see Fig. 4). These diagnostics were tested on the JanUSP laser (LLNL) and have been fielded for experiments on both the 400 fs 16 J LULI laser facility (École Polytechnique) and the 800 fs 100 J VULCAN (Rutherford Appleton Labs) laser facility. The X-ray imaging is from a K_α fluorescence buried layer as a function of depth and transport material. (In Fig. 4, "K_α fluor" denotes the buried Cu or Ti layer in the target.) In the X-ray region, we have imaged (with 10 μm resolution) the 4.5 keV line in Ti and the 8.0 keV line in Cu, as well as bremsstrahlung emission from laser interaction with the front surface, *via* a bent spherical crystal mirror. The soft XUV detector images 180 Å emission from electron heating at the rear target surface *via* multi-layer MoC-Si mirrors.

Figure 5 summarizes data from the K_α images recorded from 20 μm thick fluorescence layers following transport through Al layers. Both a typical image and

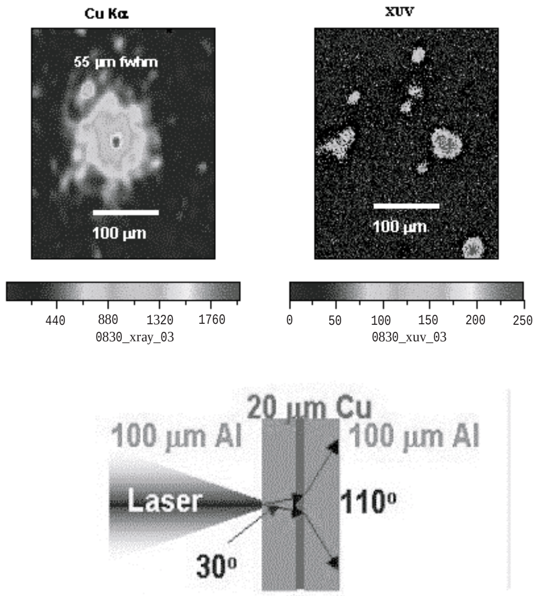

Fig. 6. The images, both K_α and XUV, recorded for a target with a Cu fluorescence layer buried within the material. The fluorescence signal is well behaved, showing a collimated beam with an appropriate width. The XUV radiation recorded on the back of the target showed a large spreading and break-up of the beam. This phenomena was recorded for every target with multiple interfaces.

a plot of the average radius at half-max intensity as a function of the thickness of Al are presented. Data from LULI are from Ti-K_α and from RAL, Cu-K_α. The images were generally in the form of a well-defined circular spot with a central peak, the spot size increasing with thickness of the transport layer. The RAL data define a truncated cone of angle 40 degrees and minimum radius 37 μm. The LULI data are similar with cone angle 54 degrees and minimum radius 34 μm. The figure shows the average image radius (μm) at half-max intensity as a function of Al thickness (μm), Cu-K_α at RAL, (filled circles) and Ti-K_α at LULI, (squares). The remarkable fact that the image radius does not converge on the known laser spot size ($\sim$10 μm) at zero aluminium thickness is discussed below. Also shown is a typical K_α image from an Al/Cu/Al sandwich target, each layer 20 μm.

Figure 6 shows a target of 100 μm Al/20 μm Cu/100 μm Al target shot at RAL. These results show simultaneously normal fluorescence image and extreme break up of XUV image. The double imaging system permitted us to observe the dramatic effects of a discontinuity in the material density on the electron transport through a slab target. This result was completely unexpected, nor predicted by any model. It was completely reproducible whenever a discontinuity was introduced into the target (such as a K_α fluor). However, for targets of only one metal (*e.g.* Al), the XUV thermal image on the back of the target showed the initial 30° cone angle without break-up. Break-up of both the K_α and XUV signal was always observed for targets in which the initial layer was any substantial thickness of a non-conductor (*e.g.*, CH).

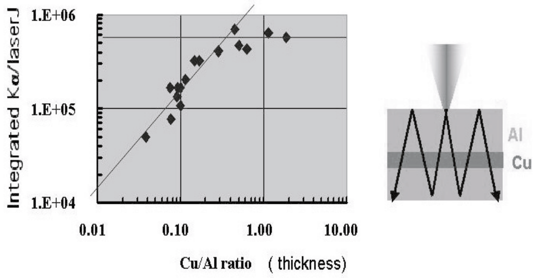

Fig. 7. The effects of "refluxing" of the electrons through the target. See text.

Figure 7 shows the K_α yield (normalized to the laser energy). These K_α data are relatively simple to interpret. They measure the flux density of electrons at the fluorescence layer. The range of the relativistic electrons is typically much greater than the target thickness; therefore the images are a summation of fluorescence produced as relativistic electrons reflux between Debye sheaths at the front and back surfaces of the target. The total fluorescence should therefore increase in the ratio of energy loss in the fluorescence to total energy loss per transit of the target. Integration of the images confirmed that this model was correct. Fluorescence excited by a divergent beam should result in an image dominated in the central region by the first pass with a large fraction of the total energy in broad wings, as seen experimentally (typically $\sim$80% of the fluorescent energy is in the wings of the distribution). Monte Carlo modeling assuming an injected electron beam of the observed minimum diameter and cone angle confirmed this general shape and suggested that the measurement of the beam size at half peak intensity gives a result close to the size on the first pass at half the peak flux density. Based on this interpretation, the fluorescence data for transport in Al therefore show a minimum electron beam diameter of about 70 μm, much greater than the 10 μm laser focal spot. We do not understand this minimal size of the apparent electron beam; the presumption is that it is related to the initial phase space in which the hot electrons are distributed.

4 Conclusions

We have presented the essential elements of the Fast-Ignitor scheme for ignition in inertial confinement fusion. Because of space constraints, we have only outlined the basic physics (see references for more detail) and we have presented representative experimental results of the measurement of fast-electron transport through dense materials. Several surprising results are highlighted, specifically the apparent large deflections at material interfaces, and the initially large electron distribution at the target interface. Some of these effects may be overcome by using the "inverted cone" target as discussed by Hatchet *et al.* [12]. We have made no attempt to review the literature on modeling (3-D PIC and Hybrid Codes [13,14]); the reader is referred to the paper by Tsakiris in this issue for a thorough discussion of the modeling of the FI scheme. One thing is evident; progress can only be made on this controlled fusion energy approach when "benchmarked" codes that can replicate calibrated experimental measurements are developed.

References

1. A. Bolye, M.H. Key, A.R. Bell, Phys. Fluids **25**, 541 (1982)
2. *Energy from Intertial Fusion* (International Atomic Energy Agency, Vienna, 1995, ISBN: 92-0-100794-9)
3. A.R. Bell, J.R. Davis, S. Guerin, H. Ruhl, Plasma Phys. Controll. Fus. **39**, 653 (1997)
4. M.J. Tabak, Hammer, M.E. Glinsky, W.L. Kruer, S.C. Wilks, J. Woodworth, E.M Campbell, M.D. Perry, Phys. Plasmas **1**, 1626 (1994)
5. M.H. Key, M. Campbell, T. Cowan, B. Hammel, S. Hatchett, E. Henry, J. Kilkenny, J. Koch, A. Langdon, B. Lasinki, R. Lee, J. Moody, M. Moran, A. Offenberger, D. Pennignton, M. Perry, T. Phillips, T. Sangster, M. Singh, R. Snavely, M. Stoyer, M. Tabak, M. Tsukamoto, K. Wharton, S. Wilks, Progress in Fast Ignition Research with the Nova Petawatt Laser, *Proceedings of the 17th IAEA Fusion Energy Conf.* (1998)
6. R. Kodoma, P.A. Norreys, K. Mima, A.E. Dangor, R.G. Evans, H.Fujita, Y. Kitagawa, K. Krushelnick, T. Miyakoshi, N. Miyanaga, S. Rose, T. Shozaki, K. Shigemori, A. Sunahara, M. Tampo, K.A. Tanaka, Y. Toyama, T. Yamanaka, M. Zepf, Nature **412**, 298 (2001)
7. M.H. Key, Nature **412**, 775 (2001)
8. M.D. Rosen, Phys. Plasmas **67**, 1690 (1999)
9. K.S. Wharton, Hatchett, S.C. Wilks, M.H. Key, J.D. Moody, V. Yanovsky, A.A. Offenberger, B.A. Hammel, M.D. Perry, C. Joshi, Phys. Rev. Lett. **81**, 822 (1998)
10. P. Mulser, Hain, Phys. Rev. Lett. **86**, 1015 (2000)
11. K. Tanaka, Study of Ultra-Intense Laser Plasma Interactions for Fast Ignitor, Invited Paper, *41st Annual Meeting of the APS DPP*, Nov. 16, 1999
12. S. Hatchett, M. Tabak, R. Turner, New Developments in Design of Cone-Focused Fast Ignition Targets, in *Proceedings of 5th Workshop of Fast Ignition of Fusion Targets*, Madeira, June 2001
13. T.P. Hughes, R.C. Clark, S.S. Yu, Phys. Rev. Spec. Top. Accel. Beams **2**, 110401 (1999)
14. M. Honda, J. Meyer-ter-Vehn, A. Pukhov, Phys. Plasmas **7**, 1302 (2000); Phys. Rev. Lett. **85**, 2128 (2000)